Physical Scaling of Water Mist Suppression of Wood Crib Fires in Enclosures

HONG-ZENG YU
FM Global
1151 Boston-Providence Turnpike
Norwood, MA 02062

ABSTRACT

A series of fire suppression experiments was conducted to evaluate the efficacy of physical scaling of water mist suppression of solid combustible fires in enclosures. Wood crib fires were used in this evaluation. The experiments were conducted in a 1:3 scale ratio based on the Froude-modeling-based scaling relationships. The parameters considered in the evaluation were: enclosure size, door opening size, water mist spray condition, fire size, fire location and fire-shielding condition. The two geometrically similar enclosures measured 1.22 × 1.22 × 1.22 m and 3.66 × 3.66 × 3.66 m. Two door opening sizes for each enclosure were tested to evaluate the ventilation effect: 0.30 × 0.61 m high and 0.61 × 0.61 m for the Scale-1 enclosure, and 0.91 × 1.83 m high and 1.83 × 1.83 m for the Scale-3 enclosure. Two wood cribs were configured for each enclosure to produce maximum free-burn fire heat release rates of 22 and 47 kW for the Scale-1 experiments, and the corresponding maxima of 340 and 740 kW for the Scale-3 experiments. Besides matching the peak heat release rates according to the scaling requirement, an attempt was also made to scale the free-burn fire growth developments. The two water mist sprays used in the previous suppression studies for gas and pool fires were employed in the present study. In each enclosure, nine ceiling-mounted nozzles were arranged in a 3 × 3 pattern with equal nozzle-to-nozzle and nozzle-to-wall spacing. The experiments showed that the fire development during free-burn and water mist application in general could be reasonably scaled for the wood crib fires in enclosures, but more sensitive to the scaling imperfection of water mist sprays as compared to the case for gas and pool fires. The thermal environment inside the enclosure was also reproduced reasonably well in different scales during water mist application as expected from Froude modeling.

KEYWORDS: physical scaling, modeling, suppression, water mist, compartment fires

INTRODUCTION

Since water mist was recognized 20 years ago as a viable alternative for fire protection [1], the fire protection industry still relies heavily on the tried-but-true, yet expensive, full-scale testing approach to develop water mist fire protection systems. The primary reason is that the industry in general has been unable to make full use of the knowledge gained from the prior protection developments for the subsequent developments, due to the lack of proven engineering tools based on first principles. This situation is also reflected in the stiff testing requirement imposed by water mist system approval standards. For instance, the ANSI standard requires that for the same type of occupancies, the same amount of full-scale fire testing has to be carried out for each of the intended building sizes for system certification [2]. In order to reduce the testing requirement, engineering tools based on first principles are essential. One of such tools is physical scaling.

The Froude-modeling-based physical scaling methodology was first developed for sprinkler applications in the early 1970s [3], where the droplet Reynolds numbers in the sprinkler sprays are typically in the range of 10 to 500. The droplet Reynolds number is defined as:

$$\mathrm{Re}_d = \frac{d\left|\vec{u}_d - \vec{u}_g\right|}{\nu_g}, \tag{1}$$

where d and $\vec{u}_d$ are the droplet diameter and droplet velocity vector, and $\vec{u}_g$ and ν_g are the gas velocity vector and gas kinematic viscosity, respectively. On the other hand, the Froude number is defined as:

$$Fr = \frac{\rho_g u_g^2}{gL(\rho_\infty - \rho_g)}, \tag{2}$$

Table 1. Froude-modeling-based scaling relationships.

Scaling parameters	Any Re_d regime	$Re_d \leq 1$	$10 < Re_d \leq 500$
Droplet drag coefficient	$\propto Re_d^{-x}$	$\propto Re_d^{-1}$	$\propto Re_d^{-1/2}$
Dimension	S^1	S^1	S^1
Time	$S^{1/2}$	$S^{1/2}$	$S^{1/2}$
All scalar parameters except droplet number density	S^0	S^0	S^0
Droplet number density	$S^{(3x-6)/(2x+2)}$	$S^{-3/4}$	$S^{-3/2}$
Velocity	$S^{1/2}$	$S^{1/2}$	$S^{1/2}$
Ventilation rate	$S^{5/2}$	$S^{5/2}$	$S^{5/2}$
Fire convective heat release rate	$S^{5/2}$	$S^{5/2}$	$S^{5/2}$
Total water discharge rate	$S^{5/2}$	$S^{5/2}$	$S^{5/2}$
Total cooling rate	$S^{5/2}$	$S^{5/2}$	$S^{5/2}$
Droplet size	$S^{(2-x)/(2+2x)}$	$S^{1/4}$	$S^{1/2}$

where ρ_∞ and ρ_g are the ambient and fire gas densities, g is gravitational acceleration, L is the characteristic dimension of the fire environment, and u_g denotes the scalar value of the gas velocity vector.

The principle of Froude modeling is that in geometrically similar environments, the following three conditions have to be preserved: 1) Froude number of the buoyancy-induced gas flow, 2) momentum transfer characteristics between the water droplets and the gas flow, and 3) droplet vaporization characteristics. Experiments conducted with gas and liquid pool fires in open space have shown that for droplet Reynolds numbers in the range of 10 and 500, the fire extinction by direct water sprays above the fire could be reasonably scaled by Froude modeling [4].

As compared to sprinkler and water sprays, water mist sprays transfer their momentum to the gas medium more quickly due to the much smaller droplets. As a result, the mist droplets tend to move closely with the gas current shortly after they are discharged, leading to low droplet Reynolds number situations, typically $Re_d \leq 1$. A comprehensive analysis of the Froude modeling shows that the scaling requirement for droplet diameter varies with the droplet Reynolds number regime in which the physical scaling is performed [5]. Table 1 presents the results from this analysis, in which the second, third and fourth columns provide respectively the general scaling relationships for any droplet Reynolds number regimes, and the regimes specifically for $Re_d \leq 1$ and $10 < Re_d \leq 500$. As shown, the droplet diameter scales with ¼-power of the scale ratio for $Re_d \leq 1$, while ½-power for $10 < Re_d \leq 500$. However, the scaling requirements for all other key parameters are identical among different droplet Reynolds number regimes except for the droplet number density.

To date, the scaling relationships pertaining to $Re_d \leq 1$ have been validated by conducting water mist fire cooling experiments in open space for methane and propylene fires in scale ratios up to 1:9 [6,7], and fire suppression experiments with propane fires and heptane pool fires in enclosures for the scale ratio of 1:3 [8,9]. In theory, the constraint to the scale ratio is that the gas flows in different scales should be comparably turbulent. However, in practice, the current nozzle technology tends to limit the scale ratio since properly scaled water mist sprays are difficult to obtain if the scale ratio is too large. Regarding fire radiation, Refs. 6-9 showed that its impact was minimal on the scaling of fire cooling and suppression under the conditions evaluated in these studies.

To explore the scaling efficacy for solid combustible fires, an experimental study of water mist suppression of wood crib fires in enclosures was performed. The data obtained in the present study is also useful for the evaluation of numerical models for water mist suppression of wood crib fires, as a first step towards the simulation of more complex solid combustible fires.

FIRE SUPPRESSION EXPERIMENTS

The experiment facility used in the previous scaling studies [8,9] was employed in the present investigation.

The facility consisted of two geometrically similar enclosures with a 1:3 scale ratio. As before, the parameters considered in the experiments were: enclosure size, door opening size, water mist spray characteristics, fire size and fire-shielding condition. The total and convective fire heat release rates produced in the Scale-1 and Scale-3 enclosures during free-burn and water mist application periods were continuously measured in each experiment respectively with a 200-kW and a 1-MW fire products collector (FPC).

Test Enclosures

The Scale-1 and Scale-3 enclosures measured 1.22 × 1.22 × 1.22 m and 3.66 × 3.66 × 3.66 m. Both enclosures were of a steel-framed structure, and respectively lined with 1.2-mm and 3.4-mm thick steel sheets to ensure that the heat loss into the enclosure walls was scaled properly. Both enclosures were completely insulated with 51 mm thick, aluminum-foil-faced insulation boards with a density of 96.2 kg/m^3 and a thermal conductivity of 0.018 W/m/K. Drainage traps were provided below each enclosure to prevent flooding on the enclosure floor.

To evaluate the effect of natural ventilation on fire suppression under water mist application, experiments were conducted with two door opening sizes for each enclosure. For the Scale-1 enclosure, the door openings measured 0.30 × 0.61 m high and 0.61 × 0.61 m; for the Scale-3 enclosure, the corresponding door openings were 0.91 × 1.83 m high and 1.83 × 1.83 m. To collect the gas effluents from the door opening to perform calorific measurements, the collection hoods of the FPCs for the Scale-1 and Scale-3 enclosures were positioned above the respective door openings. Refer to Ref. 8 for a more detailed description of these two enclosures. Figure 1 shows the Scale-1 and Scale-3 enclosures, and the gas collection hood of each FPC above the enclosure door opening.

(a) (b)

Fig. 1. Photographic illustrations: (a) the Scale-1 enclosure and the 200-kW FPC; (b) the Scale-3 enclosure and the 1-MW FPC.

Enclosure Instrumentation

To monitor the thermal environment inside the enclosure, each enclosure was instrumented with a thermocouple tree located near the left corner of the wall containing the door opening. Furthermore, heat fluxes to the enclosure's inner surfaces and radiant heat fluxes out of the door opening were also measured. These heat flux measurements confirmed the finding of Refs. 8 and 9 that the total heat loss rate to the enclosure walls and through the door opening was negligible during water mist application. Reference 8 provides some details about the heat flux instrumentation.

Each thermocouple tree consisted of eight inconel-sheathed, 26-gage, bare-bead thermocouples mounted on a vertical steel wire extending from the floor to the ceiling. To prevent direct water mist spray impingement, the thermocouple tree in each enclosure was protected with a vertical rectangular steel shield. In the Scale-1 enclosure, the thermocouples in the tree were positioned at 10, 25, 41, 51, 61, 71, 81 and 91 cm from the ceiling. In the Scale-3 enclosure, the thermocouples were positioned at the corresponding elevations of 31, 76, 122, 152, 183, 213, 244 and 274 cm below the ceiling.

Fire Products Collectors

The following measurements were made continuously in both the 200-kW and 1-MW FPCs: duct surface temperature, duct gas temperature, exhaust rate in the duct, and concentrations of CO_2, CO, O_2, total hydrocarbon and water vapor in the exhaust stream, and ambient temperature. The temperatures were measured with 30-gage K-type thermocouples. The gas concentrations were measured with Rosemount analyzers except for water vapor concentrations, which were measured with a Vaisala HMP235 sensor. The gas sampling line from the duct to the gas analyzers was heat traced to prevent condensation. Except for water vapor, other concentration measurements were corrected for time lag due to the gas transport time in the sampling line and the sensing delays of the individual analyzers [10]. Based on the gas exhaust rate and gas concentrations and temperature in the FPC and ambient, the instantaneous total and convective fire heat release rates could be determined.

The total fire heat release rate was calculated from the dry-based concentrations of CO_2 and CO and dry-based gas mass flow rate in the FPC [11]. The dry-based mass flow rate was obtained by subtracting the water vapor mass flow rate from the measured mass flow rate in the FPC. In calculating the total fire heat release rate, the heat generation per unit mass production of CO_2 and CO was taken to be 9.5 kJ/g and 5 kJ/g for wood fires [11]. The uncertainty of the heat release rate calculation due to the uncertainties of the mass-flow-rate and concentration measurements was estimated about ±8%. From this point on, all the referred fire heat release rates are total release rates.

Water Mist Sprays and Nozzle Layout

As used in the previous studies [8,9], the Hago 2.25-60P and Hago 20-60P nozzles were employed in the present experiments to produce the water mist sprays in the Scale-1 and Scale-3 enclosures. These two nozzles generated solid-cone sprays, and their spray properties are presented in Table 2.

In Table 2, $d_{v0.5}$ denotes the volume-median droplet diameter of the spray. Figure 2 shows the cumulative volume fraction versus droplet size normalized with $d_{v0.5}$ for these two nozzles, which indicates that the gross droplet size distributions of these two sprays are similar. The values of $d_{v0.5}$ and discharge rate per nozzle given in the parentheses in the table are the ideal values based on the scaling relationships presented in Table 1 for $Re_d \leq 1$. Since the Scale-3 spray's discharge rate was comparable to the ideal rate but the droplet size was larger than the ideal size, the Scale-3 spray tended to have a better penetration capability through the hot gas layer inside the enclosure. The impact of a better spray penetration on the fire suppression result will be discussed later.

Table 2. Water mist spray properties.

Scale	Nozzle	Pressure (bar)	Nominal spray angle (degree)	$d_{v0.5}$ (μm)	Discharge rate per nozzle (L/min)
1	Hago 2.25-60P	13.8	60	62	0.183
3	Hago 20-60P	41.4	60	90 (82)*	2.782 (2.853)*

Note ()*: The values in the parentheses are the ideal values based on the scaling relationships for $Re_d \leq 1$ presented in Table 1.

In each enclosure, nine nozzles were arranged in a 3 × 3 matrix with equal spacing between adjacent nozzles and between nozzles and adjacent walls, with the nozzle tips being about 32 mm below the ceiling. A high pressure pump rated 114 L/min at 69 bar was used to supply the required water discharge rates. A 100 μm filter was installed at the pump intake and a 20 μm filter was installed at the inlet of the enclosure piping system to remove particulates. The nozzle discharge pressure was monitored with a 69-bar rated pressure transducer (Trans-Metrics Model P21EA-10) at the piping manifold above the enclosure. The water temperature in the tubing above the enclosure was monitored at the ceiling center and near the right corner of the wall containing the door opening.

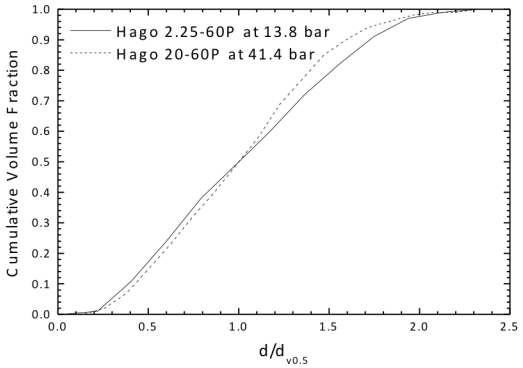

Fig. 2. The gross droplet size distributions of the Hago 2.25-60P and Hago 20-60P nozzles.

Wood Crib Fires

The Scale-1 and Scale-3 wood cribs should provide the same fire development characteristics in the enclosures. To achieve this, the following two conditions have to be met:

1) To meet the geometrical similarity requirement, all objects should be linearly scaled as closely as possible, which include the wood crib's overall dimensions and flame height.
2) To have the same burning characteristics, the ratio of air entrainment rate into the wood crib versus the burning rate should be conserved in different scales.

The flame-height-versus-fire-base-diameter is a function of $\dot{Q}^{2/5}/D$[12], where $\dot{Q}$ is the heat release rate and D is the effective diameter of the crib base. Since D has to be scaled linearly, $\dot{Q}^{2/5}$has to be also scaled linearly, leading to $\dot{Q}^{2/5} \propto H$, where H is the enclosure ceiling height. Since the fire heat release rate is proportional to burning rate, so the crib burning rate has to be proportional to $H^{5/2}$.

A previous theoretical study of non-propagating wood crib fires indicated that the air entrained into the wood crib is a function of $A_v\beta^{1/2}$ [13]， where A_v is the total opening area at the crib base and β is the distance between adjacent wood sticks. In the same study, experiments also showed that under well-ventilated conditions, the crib burning rate is proportional to the product of total crib surface area A_s exposed to the air and $b^{-1/2}$, where b is the wood stick thickness. Therefore, to reproduce the burning characteristics under both over- and under-ventilated conditions, the ratio of $A_v\beta^{1/2}/A_sb^{-1/2}$ has to be conserved in different scales, i.e., the ratio of the air supply rate to wood crib for burning and the total wood pyrolysis rate.

For square wood cribs constructed with wood sticks of square cross-section, it can be shown that

$$A_v = (\ell - nb)^2, \tag{3}$$

and

$$A_s = 4nNb\ell[1 - \frac{b}{2\ell}(n - 1 - \frac{n}{N})] \quad , \tag{4}$$

where ℓ is the wood stick length, n is the number of sticks per layer, and N is the number of layers in the wood crib.

Assuming that b, ℓ, n and N are individually proportional to the enclosure height, and applying the above two conditions for preserving the fire development characteristics in different scales, the following relationships can be obtained [14]:

$$b \propto H^{1/2}; \ell \propto H^{9/8}; n \propto H^{1/2}; N \propto H^{5/8} \tag{5}$$

To evaluate the fire size effect, two wood crib sizes were configured for each enclosure. The peak heat release rates of the two Scale-1 cribs were targeted in the range of 20-25 kW and 45-50 kW, to be in line with the fire sizes used in the previous scaling studies for the gas and pool fires [8,9]. All the cribs were made of near knob-free northern spruce pine, with a dry-based moisture content of 4-8%. After the configurations of the two Scale-1 cribs were finalized with the heat-release-rate measurements under the FPC in open space to obtain the peak heat release rates of about 22 and 47 kW, the specifications of the corresponding Scale-3 cribs were projected from the relationships given in Eq. 5. Based on the heat-release-rate measurement, fine tuning was made to the projected specifications in order to obtain the corresponding Scale-3 peak heat release rates of about 340 and 740 kW. The final specifications of the two Scale-1 and two Scale-3 wood cribs are given in Table 3, and Fig. 3 shows the larger cribs used in the Scale-1 and Scale-3 experiments.

Each experiment was started by uniformly igniting the wood crib at the base with pan fire. The pan fire for the Scale-1 cribs was prepared by soaking a layer of 3-mm thick inorganic felt paper with 35 cc of ethanol inside a 229 x 229 x 19 mm high steel pan. For the Scale-3 cribs, the steel pan was 711 x 711 x 25 mm high and the felt paper was soaked with 300 cc of ethanol. The base of each wood crib was raised about 12 mm above the pan with four metal spikes secured at the crib's four corners.

Table 3. Scale-1 and Scale-3 wood crib specifications.

Scale ID	**Nominal maximum heat release rate (kW)**	**Specifications** ***b*(mm)-ℓ (mm)-*n*-*N****
Scale 1	22	16-191-8-6
	47	16-191-6-12
Scale 3	340	27-657-16-11
	740	27-657-12-20

*See Eqs. 3 and 4 for symbol definitions.

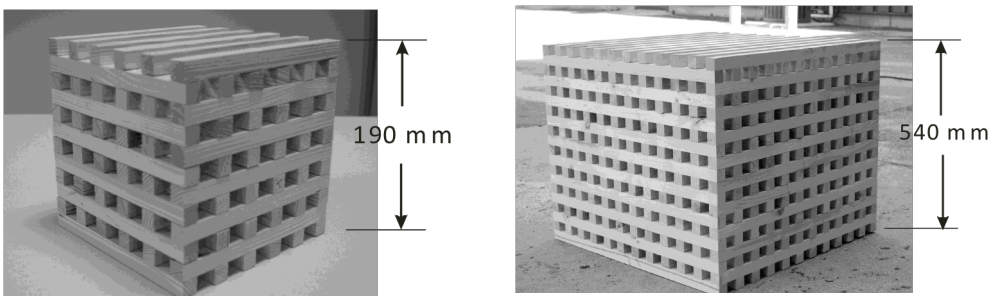

Fig. 3. The corresponding larger wood cribs used in the Scale-1 (left) and Scale-3 (right) experiments.

Figure 4 shows the heat-release-rate histories of the smaller and larger Scale-1 wood cribs free-burning in open space. In each plot, the initial hump of each test was caused by the ethanol pan fire. The incipient times of crib ignition were shifted in the plots to evaluate the reproducibility of fire development. Overall, the reproducibility for each crib configuration was reasonably good in both the growing and decaying periods. The maximum heat release rates of the smaller and larger crib fires were about 22 and 47 kW. The radiation fraction at the maximum heat release rate was measured about 0.15 for both the smaller and larger cribs.

Figure 5 shows the heat-release-rate histories of the smaller and larger Scale-3 cribs free-burning in open space, where two replicated tests were conducted for the smaller crib while only one test was conducted for the larger crib. As compared to the Scale-1 fires, the heat from the initial ethanol pan fire was not as pronounced as compared to the maximum values for both the smaller and larger Scale-3 fires. The peak heat release rates of the smaller and larger Scale-3 fires were about 340 and 740 kW respectively, corresponding closely to $3^{2.5}$ times the peaks of the respective Scale-1 fires. The radiation fraction at the peak heat release rate was measured about 0.25 for both the smaller and large wood cribs. The impact of the radiation difference between the Scale-1 and Scale-3 fires on the thermocouple temperature inside the enclosure will be discussed later.

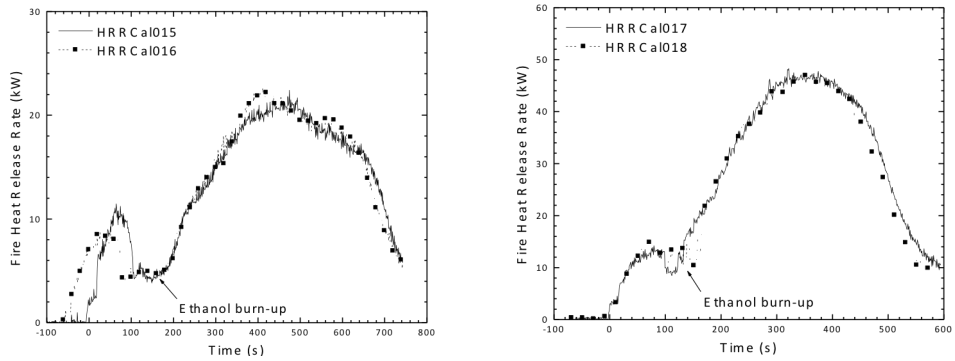

(a) (b)

Fig. 4. The Scale-1 fire-heat-release-rate histories for: (a) the smaller wood crib; (b) the larger wood crib.

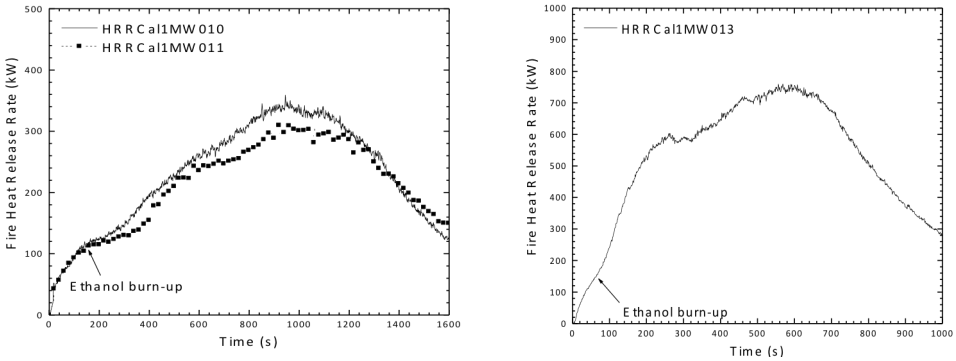

(a) (b)

Fig. 5. The Scale-3 fire-heat-release-rate histories for: (a) the smaller wood crib; (b) the larger wood crib.

Figure 6(a) compares the normalized heat-release-rate histories of the corresponding smaller Scale-1 and Scale-3 cribs, and Fig. 6(b) shows the comparison for the corresponding larger cribs, all free-burning in open space. The comparisons are made on the Scale-1 basis for both the time and fire heat release rate, i.e., heat release rate is divided by $S^{5/2}$ and time lapse is divided by $S^{1/2}$. For clarity, only one test result for each crib is presented in each figure. As shown, for the smaller cribs, the Scale-1 and Scale-3 fire developments were replicated reasonably well into the decaying period before the Scale-1 crib fire began to decay at a faster rate. For the larger cribs, the agreement was reasonably good up to the time when the peaks were reached. Although the Scale-3 crib fire began its decaying later than the Scale-1 fire, it exhibited a similar decaying rate as the Scale-1 fire.

Fire Shields and Shield Orientations

Except for a few experiments, to minimize the direct interaction between the water mist sprays and fire, the crib was protected with a metal shield consisting of a horizontal top cover welded to two opposite plates. The shield was fabricated with the same sheet metal used to construct the Scale-1 and Scale-3 enclosures. For the Scale-1 experiments, the shield's top cover measured 0.41 × 0.41 m, and the two side plates each measured 0.41 × 0.61 m high. For the Scale-3 experiments, the shield's top cover and its two side plates measured 1.22 × 1.22 m and 1.22 × 1.83 m high, respectively.

To evaluate the impact of air flow pattern from the door opening to the fire, two shield orientations were tested in the experiments. The first orientation was to align the two shield openings to the door opening; the second orientation was to rotate the shield by 90° so that the two opposite plates of the shield were aligned to the door opening.

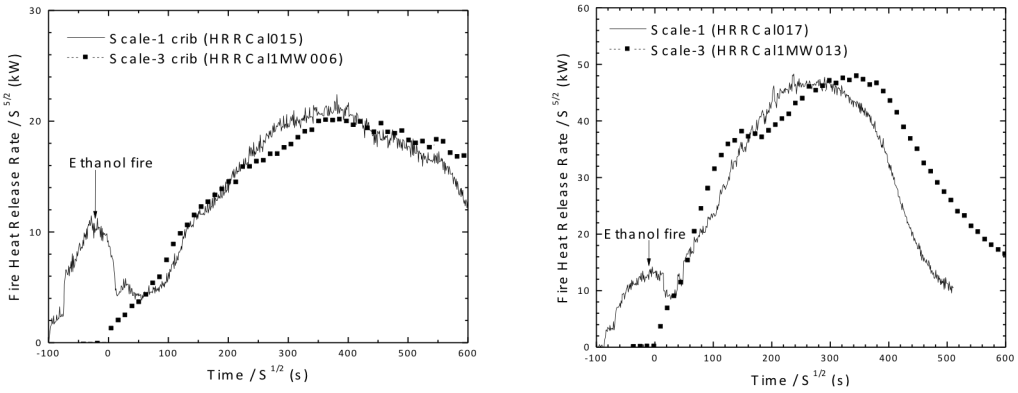

(a) (b)

Fig. 6. Comparisons of the fire heat-release-rate histories: (a) the smaller Scale-1 and Scale-3 cribs; (b) the larger Scale-1 and Scale-3 cribs.

EXPERIMENTAL PARAMETERS

The key parameters for the fire suppression experiments are summarized in Table 4. For the corresponding Scale-1 and Scale-3 experiments, the water mist application was started at the corresponding fire heat release rates (i.e., scaled with $S^{2.5}$) after ethanol was burned up, instead of the corresponding time lapse from the ethanol ignition, considering the fact that the incipient time for wood crib ignition could vary. The designated fire heat release rates at water mist application were 20 kW and 37 kW for the Scale-1 experiments, and 310 and 580 kW for the Scale-3 experiments.

Table 4. Key experimental parameters.

Scale	Enclosure size (width × depth × height) (m × m × m)	Door opening size (width × height) (m × m)	Nominal heat release rate at water mist application (kW)	Discharge pressure (bar)	Droplet median diameter (μm)	Total water mist discharge rate (L/min)
1	1.22 × 1.22 × 1.22	0.30 × 0.61 0.61 × 0.61	20, 37	13.8	62	1.65
3	3.66 × 3.66 × 3.66	0.91 × 1.83 1.83 × 1.83	310, 580	41.4	90	25.0

RESULTS AND DISCUSSIONS

Table 5 lists the 8 scenarios for the corresponding Scale-1 and Scale-3 experiments. In Scenarios 7 and 8, the shield was removed from the enclosure so that the crib fire was completely exposed to the water mist sprays. As indicated in Table 5, the experiments were conducting by placing the wood crib at the center of the enclosure floor. For the majority of the test scenarios, two tests were conducted for each scale.

Fire Development

Figures 7 and 8 show the comparisons of the fire heat release rates measured in the corresponding Scale-1 and Scale-3 experiments for all the test scenarios listed in Table 5. In each figure, the comparison is presented on

Table 5. Test scenarios.

Scenario	Crib location on floor	Crib size		Door opening size		Shield openings facing door opening?
		Scale 1	Scale 3	Scale 1	Scale 3	
1	Center	Smaller	Smaller	Larger	Larger	Yes
2	Center	Larger	Larger	Larger	Larger	Yes
3	Center	Smaller	Smaller	Smaller	Smaller	Yes
4	Center	Larger	Larger	Smaller	Smaller	Yes
5	Center	Smaller	Smaller	Smaller	Smaller	No
6	Center	Larger	Larger	Smaller	Smaller	No
7	Center	Smaller	Smaller	Smaller	Smaller	No Shield
8	Center	Larger	Larger	Larger	Larger	No Shield

the Scale-1 basis, i.e. time is normalized by $S^{1/2}$ and heat release rate is normalized by $S^{5/2}$. The Scale-1 results are shown in lines and Scale-3 results are in symbols. To delineate the comparison of fire development during free-burn and water mist application periods, the plots in each figure were aligned at the start of water mist application. As shown in the next section, the thermocouple temperatures inside the Scale-3 enclosure in general were higher than those inside the Scale-1 enclosure before the start of water mist application, due to the fact that the Scale-3 fires were relatively more radiative. However, the advantage of higher temperature on droplet vaporization at the beginning of water mist application disappeared quickly due to the fact that the subsequent enclosure temperatures were reproduced closely in the Scale-1 and Scale-3 experiments, resulted from the negligible direct heat loss to the enclosure walls and door opening during water mist application, as was also found in the previous studies [8,9].

In Scenarios 1 and 2, the larger door opening was used and the fire shield openings were facing the door opening. In general, the Scale-3 fire was more responsive to the water mist application right after the application started. This could be attributed mainly to the better penetration capability of the Scale-3 sprays to the enclosure floor as described earlier. However, after the fire was weakened sufficiently so that the spray penetration conditions in the Scale-1 and Scale-3 experiments were comparable relative to the respective fire intensities, the normalized fire intensities tended to become more agreeable.

Scenario 3 was identical to Scenario 1, except that the smaller door openings were used in the Scale-1 and Scale-3 experiments. Both the Scale-1 and Scale-3 fires were suppressed right after the water mist application, but subsequently regained some of their intensities throughout the experiments with large fluctuations. Overall, the smaller Scale-1 fire was reproduced reasonably well in the Scale-3 experiments.

Scenario 4 was identical to Scenario 2, except that the smaller door openings were used. The Scale-1 fire was not suppressed right after the start of water mist application, similar to that observed in Scenario 2. Apparently, the suppression propensity of the Scale-1 fire by the Scale-1 sprays was little affected by changing the door opening from the larger to the smaller size. On the other hand, the Scale-3 fire reacted to the suppression action quickly right after the start of water mist application, although re-gained its intensity subsequently in the course of the experiments. This may be reasoned in the following. As the door opening is reduced, the degree of air vitiation tends to increase in the enclosure under fire and water mist application conditions, leading to a weaker fire. If the weakening is sufficient just for the Scale-3 spray (i.e., stronger relative to the Scale-1 spray) but not for the Scale-1 spray to provide sufficient mixing of fire gases and water mist in the enclosure, the Scale-3 fire suppression result is then expected to be more pronounced.

Scenarios 5 is the same as Scenario 3, except that the shield was turned 90^o so that its two openings no longer faced the door opening. With the smaller door opening plus the shield's vertical plates now blocking the direct air flow from the door opening to the fire, the fire tended to be weakened further from that in Scenario 3, leading to a better mixing inside the respective enclosures for both the Scale-1 and Scale-3 sprays. As a result, both the smaller and larger fires were suppressed quickly after water mist application in the Scale-1 and Scale-3 experiments. Overall, the development of the smaller Scale-1 fire was reproduced reasonably well in the corresponding Scale-3 experiments.

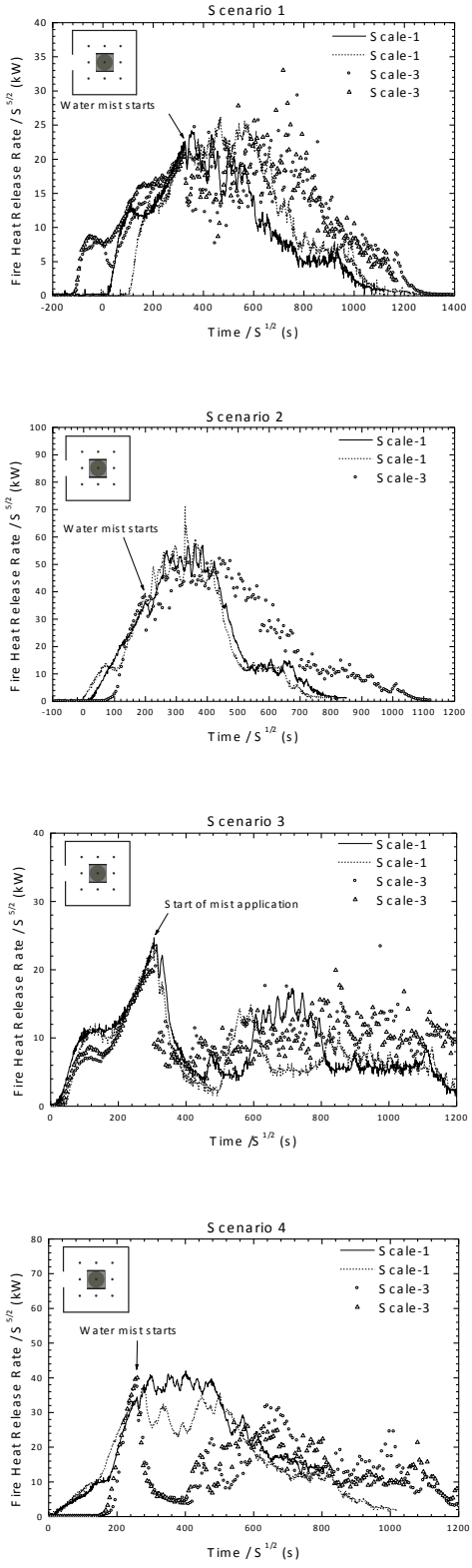

Fig. 7. Comparisons of Scale-1 and Scale-3 fire developments for Scenarios 1–4.

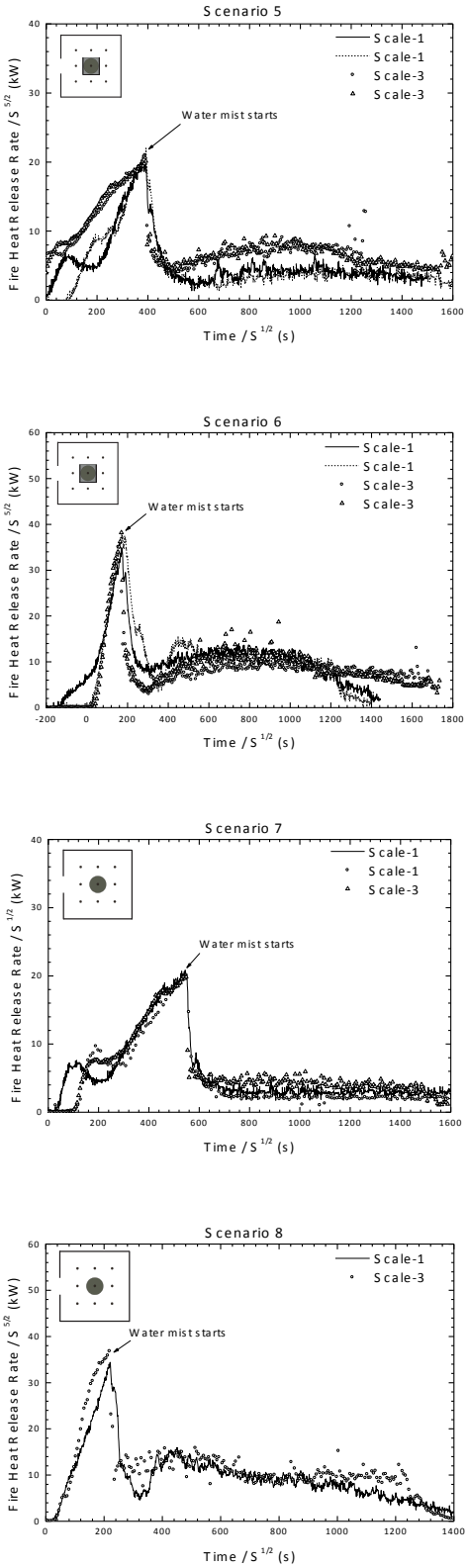

Fig. 8. Comparisons of Scale-1 and Scale-3 fire developments for Scenarios 5–8.

Scenario 6 is the same as Scenario 4, except that the shield was also turned 90^o so that its two vertical plates were aligned to the door opening. With the smaller door opening and the direct air flow from the door opening to the fire blocked, the larger wood crib fires were suppressed quickly in both the Scale-1 and Scale-3 experiments. Overall, the Scale-1 fire was reproduced quite well in the free-burn and water-mist-application periods in the Scale-3 experiments.

In Scenarios 7 and 8, the fire shield was removed. The smaller wood cribs and smaller door openings were used in Scenario 7, while the larger wood cribs and larger door openings were employed in Scenario 8. Without the shield, the fire was completely exposed to the water mist sprays. In these two scenarios, both the Scale-1 and Scale-3 fires were quickly suppressed at the time of water mist application, and remained at low intensity levels till the end of experiments. Overall, the fire developments in both scales were reproduced reasonably well.

Thermocouple Temperatures

It has been mentioned earlier that the Scale-3 fires were more radiative than the Scale-1 fires. As a result, the thermocouple temperature inside the enclosure during the free-burn period was expected to be higher in the Scale-3 experiments than in the corresponding Scale-1 experiments. During water mist application, the heat loss to the enclosure surfaces was expected to be insignificant due to the rather uniform temperature inside the enclosure, and the heavily attenuated heat radiation from the fire [8]. Therefore, the fire energy available for heating the contents inside the Scale-1 and Scale-3 enclosures tended to conform more closely to the Froude scaling requirement after water mist application, provided that the normalized instantaneous Scale-1 and Scale-3 heat release rates were comparable. As a result, a better temperature agreement between the corresponding Scale-1 and Scale-3 experiments during water mist application than during the free-burn period was expected based on the Froude modeling.

To illustrate the above expectation, Figure 9 presents the thermocouple temperatures measured in the corresponding Scale-1 and Scale-3 experiments for Scenarios 1 and 7, where the normalized heat release rates were comparable after water mist application. During free-burn, the thermal stratification from ceiling to floor was significant in both the Scale-1 and Scale-3 experiments, and the thermocouple temperatures in the Scale-3 experiments generally were higher than those in the corresponding Scale-1 experiments at the corresponding elevations inside the enclosure, as expected. After water mist application, the thermal stratification began to collapse. In general, the stratification collapsed more quickly in the Scale-3 experiments, indicating that the mixing of the contents inside the enclosure by the Scale-3 sprays was more effective. Eventually the temperatures at different elevations converged to around a lower value and then varied with time. Overall, the temperature during water mist application was reproduced reasonably well in the Scale-1 and Scale-3 experiments.

The above fire suppression results show that reproducing the fire environment inside the enclosure alone did not always lead to exact fire suppression scaling results for wood cribs. For deep-seated solid combustible fires like wood crib fires, one of the key suppression requirements is to deliver sufficient water to the fire source. This was reflected in the generally better fire suppression results in the Scale-3 experiments, due to the relatively stronger Scale-3 spray. Weakening the fire by reducing the door opening size and/or blocking the direct air flow from the door opening to the crib tended to lessen the impact of the spray penetration disparity, resulting in more favorable scaling results.

CONCLUSIONS

A series of fire suppression experiments was conducted with wood crib fires in two geometrically similar enclosures of 1:3 ratio, to evaluate the efficacy of applying Froude-modeling-based scaling relationships to water mist suppression of solid combustible fires. The parameters considered in the evaluation were: enclosure size, door opening size, water mist spray condition, fire size and fire-shielding condition. The experiments showed that the fire development in terms of heat release rate in general could be reasonably reproduced in the Scale-1 and Scale-3 enclosures, provided that the penetration capability of water mist sprays relative to fire intensity was comparable. The thermocouple temperatures inside the Scale-3 enclosure in general were higher than those inside the Scale-1 enclosure before the start of water mist application, due to the fact that the Scale-

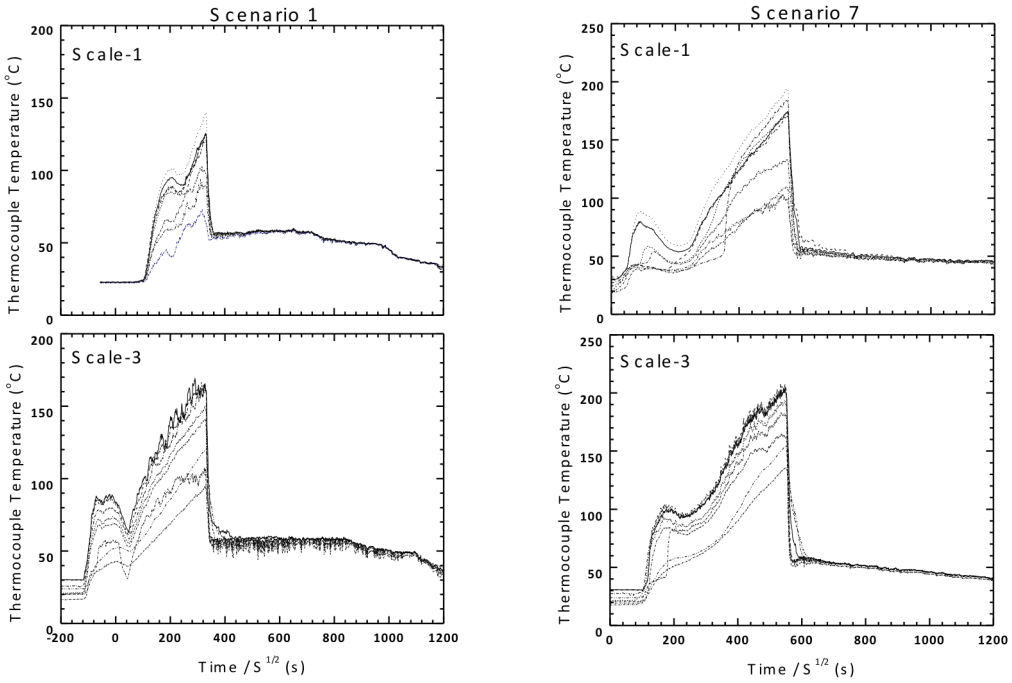

Fig. 9. Thermocouple tree temperatures measured in the Scale-1 and Scale-3 experiments for Scenarios 1 and 7 at elevations ranging from 10 to 91 cm below the ceiling in the Scale-1 enclosure, and 31 to 274 cm below the ceiling in the Scale-3 enclosure.

3 fires were relatively more radiative. However, the advantage of higher enclosure surface temperature on droplet vaporization at the beginning of water mist application, thus a more pronounced initial fire suppression, tended to disappear quickly due to the fact that the subsequent enclosure temperatures were reproduced closely in the Scale-1 and Scale-3 experiments. The good temperature agreement during water mist application was resulted from the negligible heat loss to the enclosure walls and door opening, due to the rather uniform temperature inside the enclosure, and the heavily attenuated heat radiation from the fire. As a result, the fire energy available for heating the contents inside the Scale-1 and Scale-3 enclosures tended to confirm more closely to the scaling requirement during water mist application. As compared to the previous pool fire study [9], the reproduction of wood crib fire development in different scales was more sensitive to the scaling imperfection of water mist sprays. This is due to the fact that, in addition to reproducing the fire environment condition, the other key suppression parameter for deep-seated solid combustible fires is the amount of water actually delivered to the fire source.

REFERENCES

[1] Mawhinney, J.R., "Water Mist Fire Protection Systems," *Fire Protection Handbook (20th ed)*, Cote A.E. (ed.), National Fire Protection Association, Quincy, MA 02269, 2008, p. **16**/135.

[2] "Water Mist Systems for Fire Protection," American National Standards Institute, ANSI FM5560-2007, New York, NY 10036, 2007.

[3] Heskestad, G., (1975) Physical Modeling of Fire, Fire & Flammability 6:254-273.

[4] Heskestad, G., (2003) Extinction of gas and liquid pool fires with water sprays, Fire Safety Journal 38(2003): 301-317. http://dx.doi.org/10.1016/S0379-7112(02)00085-1

[5] Yu, H-Z, (2012) Froude-modeling-based general scaling relationships for fire suppression by water sprays, Fire Safety Journal 47(2012): 1-7. http://dx.doi.org/10.1016/j.firesaf.2011.09.006

[6] Jayaweera, T.M. and Yu, H-Z (2008) Scaling of fire cooling by water mist under low drop Reynolds number conditions, Fire Safety Journal 43(2008): 63-70. http://dx.doi.org/10.1016/S0379-7112(02)00085-1

[7] Yu, H-Z, "A Revisit of Froude-Modeling-Based Physical Scaling of Fire Suppression by Water Sprays," *Suppression and Detection Research and Applications: A Technical Working Conference (SUPDET 2009)*, International Plaza Resort & Spa, Orlando, Florida, February 24-27, 2009.

[8] Yu, H-Z, Zhou, X. and Ditch, B.D., "Experimental validation of Froude-modeling-based physical scaling of water mist cooling of enclosure fires," *Fire Safety Science - Proceedings of the ninth International Symposium*, International Association for Fire Safety Science, 2008, pp. 553-564.

[9] Yu, H-Z, "Physical Scaling of Water Mist Suppression of Pool Fires in Enclosures," *Fire Safety Science – Proceedings of the tenth International Symposium*, International Association for Fire Safety Science, 2011, pp. 145-158.

[10] Croce P.A., (1976) A method for improved measurement of gas concentration histories in rapidly developing fires, Combustion Science and Technology 14:221-228. http://dx.doi.org/10.1080/00102207608547530

[11] Tewarson A., "Generation of heat and chemical compounds in fires," *The SFPE Handbook of Fire Protection Engineering (3rd ed),* DiNenno P.J. (ed.), National Fire Protection Association, Quincy, MA 02269, 2002, p. **3**/82.

[12] Thomas, P.H., Webster, C.T. and Raftery, M.M., (1961) Some Experiments on Buoyant Diffusion Flames, Combustion and Flame, 5:359-367.

[13] Block, J.A., "A Theoretical and Experimental Study of Nonpropagating Free-Burning Fires," *Proceedings of Thirteenth Symposium (International) on Combustion*, The Combustion Institute, 1971, pp. 971-978.

[14] Croce, P.A. and Xin, Y., (2005) Scale modeling of quasi-steady wood crib fires in enclosures, Fire Safety Journal 40 (2005): 245-266. http://dx.doi.org/10.1016/j.firesaf.2004.12.002